INSTITUT FÜR AERODYNAMIK UND GASDYNAMIK

IAG

DIREKTOR: PROF. DR.-ING. SIEGFRIED WAGNER
Universität Stuttgart · Pfaffenwaldring 21 · 7000 Stuttgart 80 · Telefon (0711) 685-34 01 · Telefax (0711) 685-34 38

INFLUENCING TRANSITION ON AIRFOILS

D. Althaus

Stuttgart 1981
vorgetragen beim 17. OSTIV-Kongress Paderborn 1981

Influencing Transition on Airfoils

D.Althaus *

Presented at the XVII OSTIV Congress, Paderborn,W.-Germany(1981)

The performance of airfoils mainly depends on the position and the sort of transition from the laminar to the turbulent boundary layer. In dependence of the angle of attack or lift coefficient and Reynoldsnumber, they define the initial conditions for the turbulent boundary layer. In the range of Reynoldsnumbers for soaring, which is between 0.5 and 3.5 millions, transition takes place in the separated laminar boundary layer. The turbulent boundary layer then attaches to the surface and a so-called laminar separation bubble is formed. At higher Reynoldsnumbers, transition occurs in the boundary layer attached to the wall. So initial conditions for the turbulent boundary layer can be quite different. According to the lay-out of the pressure-rise for the turbulent boundary layer, a variation of the initial conditions can imply early separation of the boundary layer. In designing an airfoil proper handling of boundary layer transition at all flight conditions is a primary aim. Fig.1 shows the velocity distribution for the Liebeck R 1511 airfoil. This is an example for an airfoil without any provision for influencing boundary layer transition. The stable laminar boundary layer suddenly must sustain the sharp turbulent pressure-rise. Oilflow pictures, taken at the wind tunnel tests, showed a laminar separation bubble with a length of 30 % of chord forming at the beginning of the pressure-rise. By means of a trip wire, which was positioned at $x/c = 0.3$, the instability of the laminar boundary layer was increased resulting in a rather small separation bubble. The drag could be appreciably

---

* Institut für Aero- und Gasdynamik der Universität Stuttgart

reduced as is demonstrated in Fig.2. This example shows that handling of transition is very essential. Some means for controlling shall be demonstrated.

Transition can be achieved by shaping of the contour. F.X.Wortmann /1/ shows that it is possible to control transition by inserting a so-called instability range with a flat negative velocity gradient between the positive and the negative velocity gradients. The velocity distributions of the 13 per cent thick airfoil WP 2 at an angle of attack of $\alpha = 1.3^{o}$, shown in Fig.3, have no instability ranges. Wind tunnel tests revealed laminar separation bubbles at the beginning of the pressure-rise as marked in the figure. The velocity distribution of the upper side was modified with an instability range beginning at 30 per cent of chord developing a laminar boundary layer with constant formparameter. This velocity distribution is shown on the figure by the broken line called WP 2 MOD. The contour of the wind tunnel model WP 2 was modified accordingly. At a chord length of 500 mm, the change in contour had a maximum of 1 mm. The lift drag polars for the original model WP 2 and the modified model WP 2 MOD are shown in Fig.4. The polar of the WP 2 airfoil for Re = 0.7 millions shows the form of the laminar drag bucket characteristical for laminar separation bubbles. By the application of the instability range on airfoil WP 2 MOD, the drag is maintained constant within the whole laminar bucket. At higher Reynoldsnumbers, the reduction of drag by the instability range is small as is to be expected, at the upper end of the laminar bucket the drag even increases. This is no disadvantage as at an airfoil in flight with high Reynoldsnumbers only the medium and the low range of the laminar bucket is used.

Another example for the use of the instability range is shown in Fig.5. The symmetrical airfoil IS 30 A/150 with a thickness of 15 per cent is designed with an instability range from 40 to 70 per cent of chord. A new instability range beginning at about 45 per cent with a somewhat higher formparameter and a resulting stronger pressure gradient was calculated. The shape of the upper side of the wind tunnel model was modified accordingly. Fig.6 shows the lift drag polars for the symmetrical airfoil and the airfoil IS 30 A/150 MOD with modified upper side. A small reduction of drag was achieved at negative angles of attack for small Reynoldsnumbers. At high Reynoldsnumbers and positive angles of attack, the drag coefficient is enlarged i.e. the pressure gradient of the instability range is too high, transition occurs too early along the instability range.

Distinct disturbances at the surface of the airfoil reveal a further possibility to control transition. They also increase the instability of the laminar boundary layer. Roughnesses used in early times are difficult to produce and to fix at the airfoil surface. The installation of tripwires is also problematic. Both devices are not suited for the use on an airplane. The author uses transition trips consisting of self-sticking Mylar-film with digged-in bumps with a spherical or grainlike form. Strips of any width are easily produced with a modified sewing machine. The needle is replaced by one with a ball-shaped tip. The height of the bumps and their distance can be varied. For larger distances the film is transported by a step motor. These transition trips are easily reproduceable and can be installed anywhere on an airfoil surface.

Recently blowing of air was again claimed to be a favourable transition device. Small amounts of air are blown through

small holes vertically to the surface. The disadvantage of this method is the laborious and expensive installation of the holes and the air supply. The holes can be obstructed by dirt and rain. The only advantage of this installation could be, that blowing might be turned off when it is not afforded. But this is difficult to achieve because circulation of air induced by the spanwise pressure gradients must be avoided.

Some examples for the application of transition devices: the lift drag polars for the airfoil WP 2 are shown in Fig.7. At this airfoil no instability range is provided for (see Fig.3). Strips with sandroughness were installed on the upper side between 60 and 62 per cent of chord, at the lower side between 72 and 74 per cent i.e. at the beginning of the pressure-rise or the laminar separation bubble. At smaller Reynoldsnumbers the drag is reduced, but at the higher Reynoldsnumbers drag penalities have to be allowed for. Position and height of the roughness was not optimized in this case. In behalve of clarity the origins for the different Reynoldsnumbers have been shifted on Fig.7.

Fig.8 demonstrates lift-drag polars of a flapped airfoil at a Reynoldsnumber of 2 millions. At a flap-setting of $\beta = -5^{\circ}$, an appreciable drag reduction could be gained by a Mylar-film tripping device as mentioned above on the lower surface of the airfoil at 80 percent of chord that means just before the hinge of the flap. The velocity distribution in Fig.9 reveals a sharp transition to the turbulent pressure-rise at the hinge of the flap resulting in a laminar separation bubble. By the transition trip, this bubble is minimized and thereby the drag reduced.

Fig.10 shows a lift drag polar of the flapped airfoil HQ 19/1398 at a Reynoldsnumber of 2.5 millions and a flap setting of $\beta = -10^{\circ}$. The wind tunnel model was fitted with a blowing installation mentioned above. The broken line holds for a measurement with the holes sealed by a thin film. By blowing of a small amount of air a gain in drag could be achieved as shown by a full line. Exactly the same polar was attained when the holes were sealed by a thin film having a bump with a height of 0.5 mm just over each hole. This device is of course essentially cheaper and simpler than the complicated installation for blowing. The velocity distribution for this airfoil looks like that shown in Fig.9. By blowing of air or by triggering through the bumps, boundary transition was forced at the hinge of the flap resulting in an only small laminar separation bubble.

Triggering transition by blowing or by disturbances at the surface can be successfully applied, where thick and long laminar separation bubbles have to be deminished or removed. Large separation bubbles form when a relative stable laminar boundary layer should sustain an abrupt transition to a sharp pressure-rise. This is the case on airfoils with long laminar lengths or on airfoils designed for high lift which have high super-velocities at the upper side. To reach the trailing edge velocity with a tolerable pressure gradient for the turbulent boundary layer the recovery has to begin rather early.

On airfoils with velocity distributions showing a light pressure-rise within the laminar range or some sort of instability range, only small laminar separation bubbles are formed. Experience shows that a reduction of drag is difficult to achieve by disturbances on the surface or

blowing in this case. Either there is no effect or the drag is even increased. A proper instability range in the velocity distribution provided at the design of the airfoil will be preferable.

Boundary layer transition can be affected by an unwanted tripping device: the insects. During summertime insects are collected on the airfoil nose and form roughnesses for the laminar boundary layer. From each roughness, which is high enough, a wedge-shaped turbulent boundary layer emerges. After a short length these wedges form a uniform turbulent boundary layer along the span of the wing. This early transition in addition with the higher wall-shear of the turbulent boundary layer results in an increase of drag. At the beginning of the pressure-rise there is now a thick turbulent boundary layer which will separate early. This again results in a reduction of the lift coefficient.

Calculations of the performance of airplanes base on the assumption of ideal smooth airfoils. What losses in performance have to be expected by roughness due to insects? Johnson /3/ made flight tests on sailplanes with artificial insects. He used small pieces of tape with a length of 5 x 5 mm and a height of 0.25 mm. A row of these "bugs" was fixed on the airfoil nose in a distance of 150 mm. Some 12 mm above and below the airfoil nose further rows of bugs were fixed in alternating form. Thus 1 m of span was fitted with 20 bugs. This surely does not correspond with reality, but some standard was defined.

To get comparable wind tunnel tests on airfoils with insects, a pattern for insects on airfoil noses was accepted. 10 mm wide strips of Mylar-film, 0.2 mm thick, with bumps in a distance of 30 mm and 0.5 mm high are used. One of

these strips is fastened on the airfoil nose in such a way that the bumps are directly in the nose line. One strip is fixed tightly at the lower side and two further strips tightly on the upper side of the airfoil nose in such a way that thebumps are shifted spanwise half a distance from strip to strip. This results in about 130 bugs per meter span. This pattern is thought to confirm with reality. The advantage of this method is that the strips are easy to produce and to fix, the pattern is easily reproduceable. It should not be too difficult to set it all along a wing of an airplane.

Tests on airfoils with this bug pattern provide an information about the sensibility of the distinct airfoils with equal disturbances. Fig.11 shows the lift drag polars of the airfoil FX 61-163 with artificial insects according to the pattern described above. Results from the clear airfoil are drawn in dashed lines for comparison. In the upper range of the low drag bucket an essential increase in drag results from the bugs. At lower lift coefficients the increase in drag is larger for Re = 2.5 millions than for Re = 1 million. As Fig.12 shows the influence of roughness due to insects is even more drastically on airfoils with flaps. Tests on the airfoil FX 67-K-150/17 are shown in Fig.12 as an example. In comparison to the results on the clear airfoil substantial drawbacks show in the lower range of the bucket but even more at the upper end of the bucket. The slope of the lift coefficient has flattened compared with the clear airfoil results, the maximum lift is nearly the same for both cases. Tests on the airfoil FX 62-K-131/17 in Fig.13 show similar results for Re = 1 million. At Re = 2.5 millions the increase in drag ist somewhat smaller than in the former example. In the upper range of the bucket the drag is smaller for Re = 2.5 millions than for Re = 1 million.

The drawbacks by roughness due to insects are smaller for the unflapped airfoil FX 61-163 than for the flapped ones. The pressure-rises for the airfoil FX 61-163 on both sides are flatter than those for flapped airfoils at positive or at negative flap-settings. If, owing to the roughness due to insects, transition is forced near the airfoil nose, the turbulent boundary layer at the beginning of the pressure-rise is essentially thicker than for the clear airfoil. Flapped airfoils show premature separation by this reason.

Performance of sailplanes with these airfoil-bug-polars: for comparison performances of two sailplanes with a span of 15 m were evaluated with the airfoil polars in Fig.11 and Fig.12. Fig.14 shows the polar for straight flight and circling for a 15 m FAI-sailplane with a clear wing and wing with bugs, with the flapped airfoil FX 67-K-150/17. Fig. 15 demonstrates the polars for a 15 m standard-sailplane with the airfoil FX 61-163. In Table 1, some figures from these performance calculations are collected. In addition the relativ penalities caused by the insects are demonstrated. The losses in performance are essentially larger for the flapped airplane. These calculated penalities are somewhat larger than those measured by Johnson owing to his rather crude bug pattern.

At the wind tunnel tests all airfoils were tested with the same bug pattern. However, from experience we know, that different airfoils collect not the same number of bugs under similar conditions. The impingement and rupture of insects depends on the form of the airfoil nose, the position of the stagnation point and the airfoil thickness. Essential factors for the rupture of the insects are the velocity and the angle of impingement.

In order to get more information about the vulnerability of different airfoils by insects some information should be gathered by evaluating the bug pattern on wings after flight. A thin Mylar-film could be adhered to the wing nose. When the airfoil nose line is marked on the film, the distribution of insects can easily be evaluated, when the film is detached after the flight. The film with the bugs even could be fixed on a wind tunnel model of the same airfoil to get wind tunnel results with the real pattern.

These tests and examples show what detrimental losses in performance are caused by the contamination of insects. Just the airfoils breeded for high performance reveal to be the most vulnerable ones. Perhaps some dispense with performance of the clear airfoil and thereby a smaller loss by insects would be a compromise. F.X.Wortmann /4/ showed already in 1963 that contamination by insects can be avoided by the use of an elastic airfoil nose. The large expenditures,which have to be made for an airplane with high performance , afford to look for a way that these performances are guaranteed to a certain degree even with roughness due to insects.

Literature

/1/ F.X.Wortmann: Experimentelle Untersuchungen an neuen Laminarprofilen für Segelflugzeuge und Hubschrauber, ZfW 5 (1957)

/2/ F.X.Wortmann: Boundary Layer and Flow Control Pergamon-Press (1961)

/3/ R.Johnson: Flightest Evaluations Soaring (Soaring Society of America)

/4/ F.X.Wortmann: Über eine Möglichkeit zur Vermeidung der Insektenrauhigkeit 9.OSTIV-Kongress (1963),Argentinien Schweizer Aero-Revue 11 (1963)

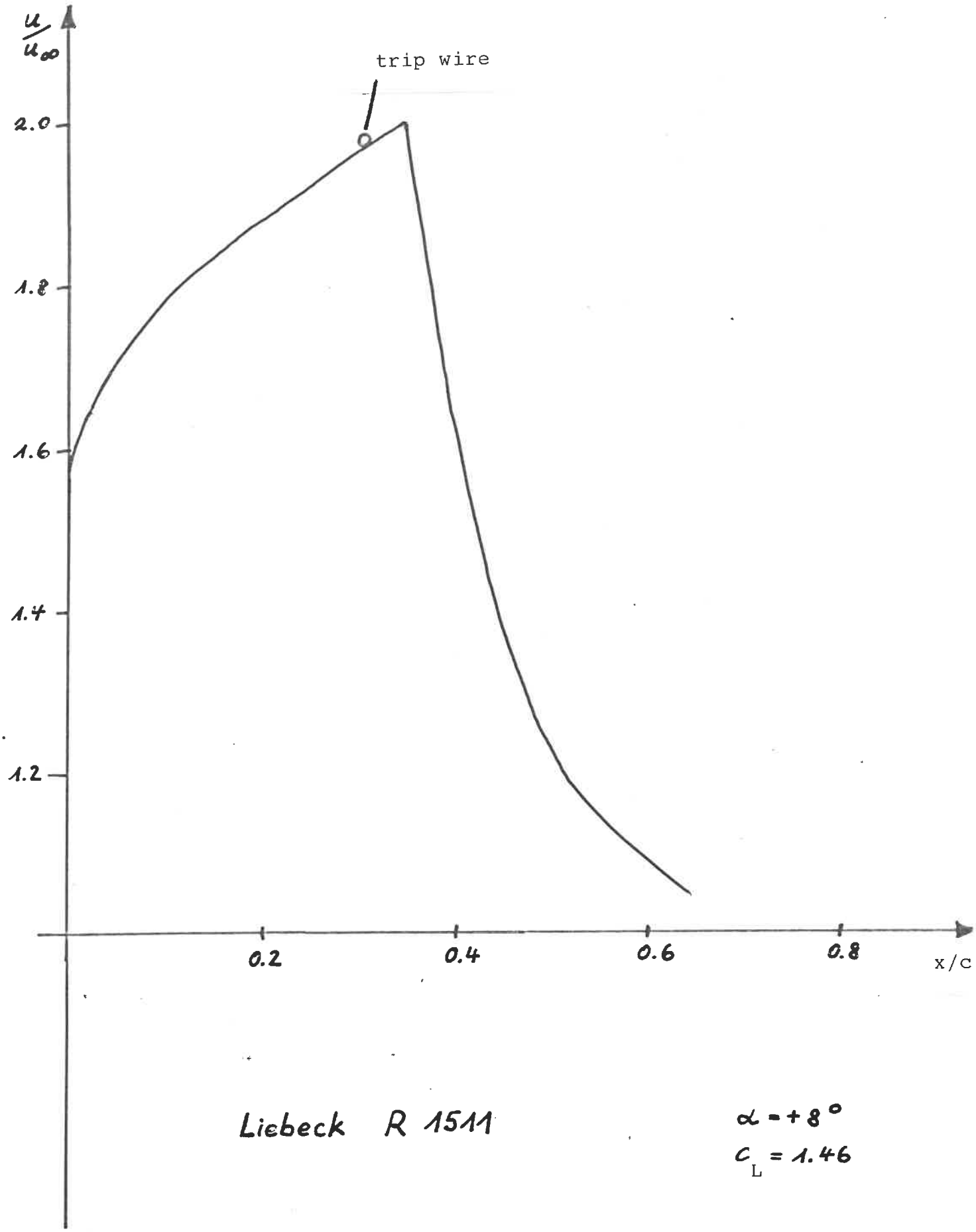

Liebeck R 1511

$\alpha = +8°$

$c_L = 1.46$

Fig. 1

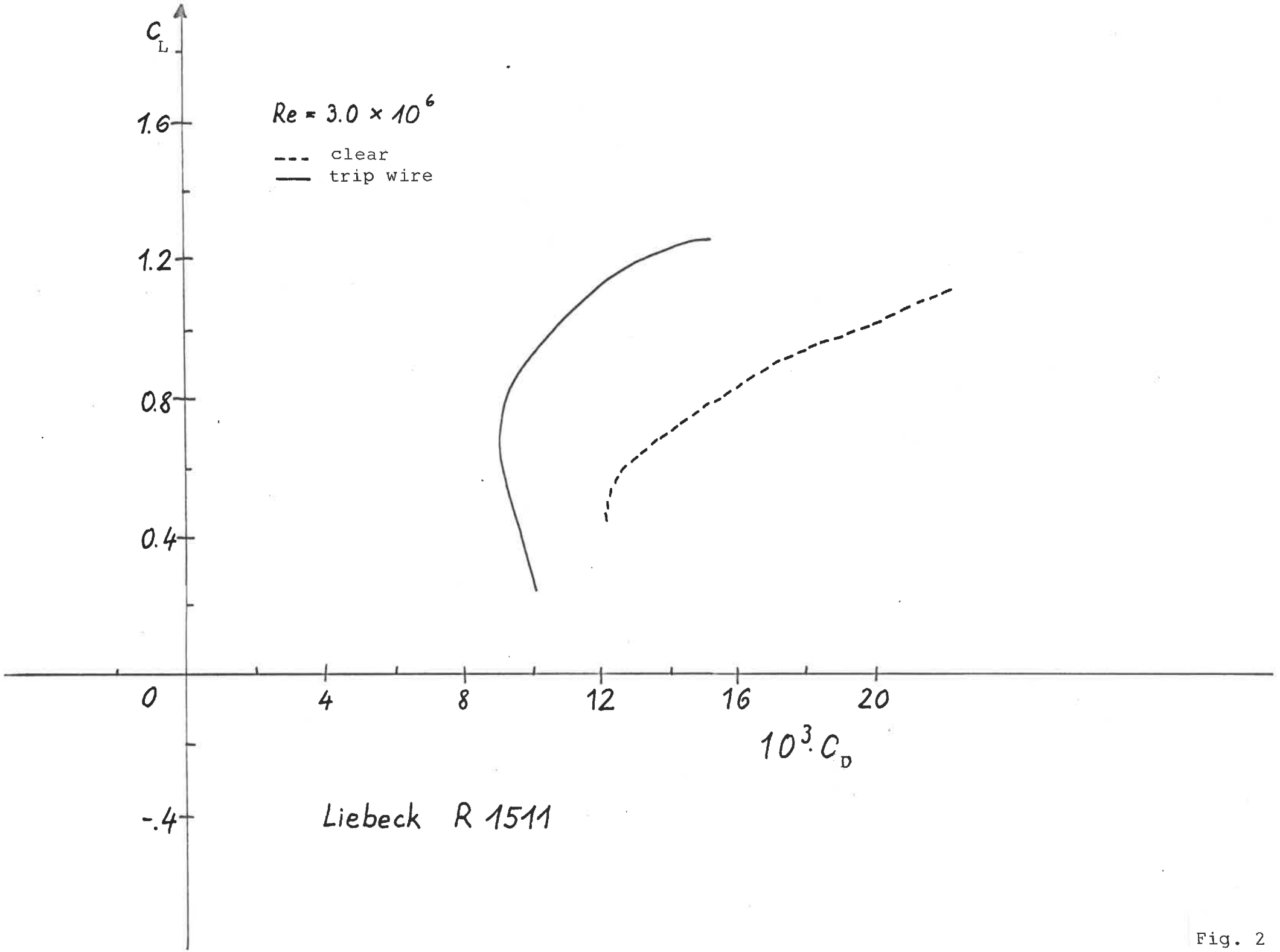
C_L
1.6
1.2
0.8
0.4
-.4
0
4
8
12
16
20
$10^3 . C_D$
$Re = 3.0 \times 10^6$
clear
trip wire
Liebeck R 1511

Fig. 2

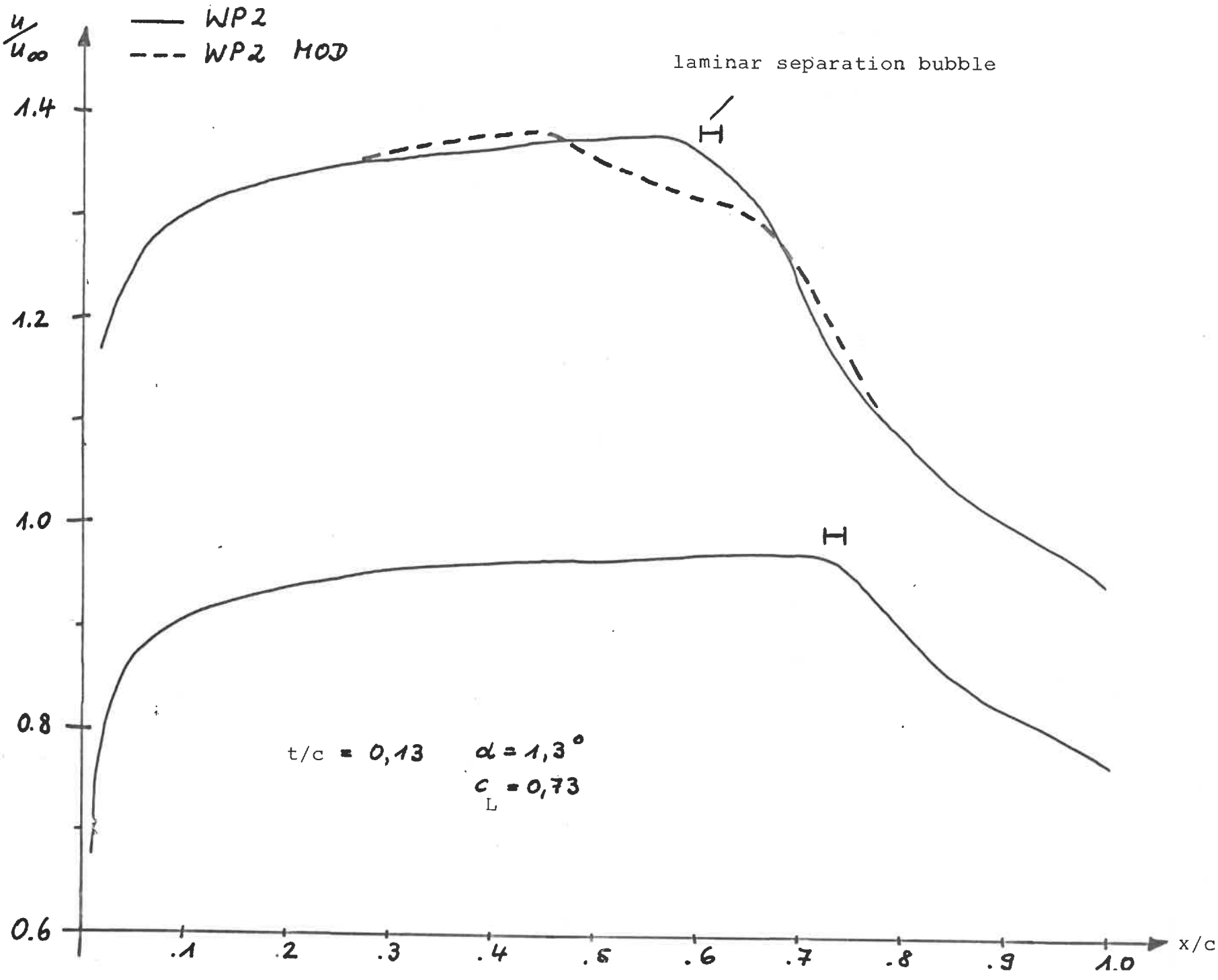
u/u∞
WP2
WP2 MOD
laminar separation bubble
H
H
1.4
1.2
1.0
0.8
0.6
t/c = 0,13
α = 1,3°
c_L = 0,73
.1
.2
.3
.4
.5
.6
.7
.8
.9
1.0
x/c

Fig. 3

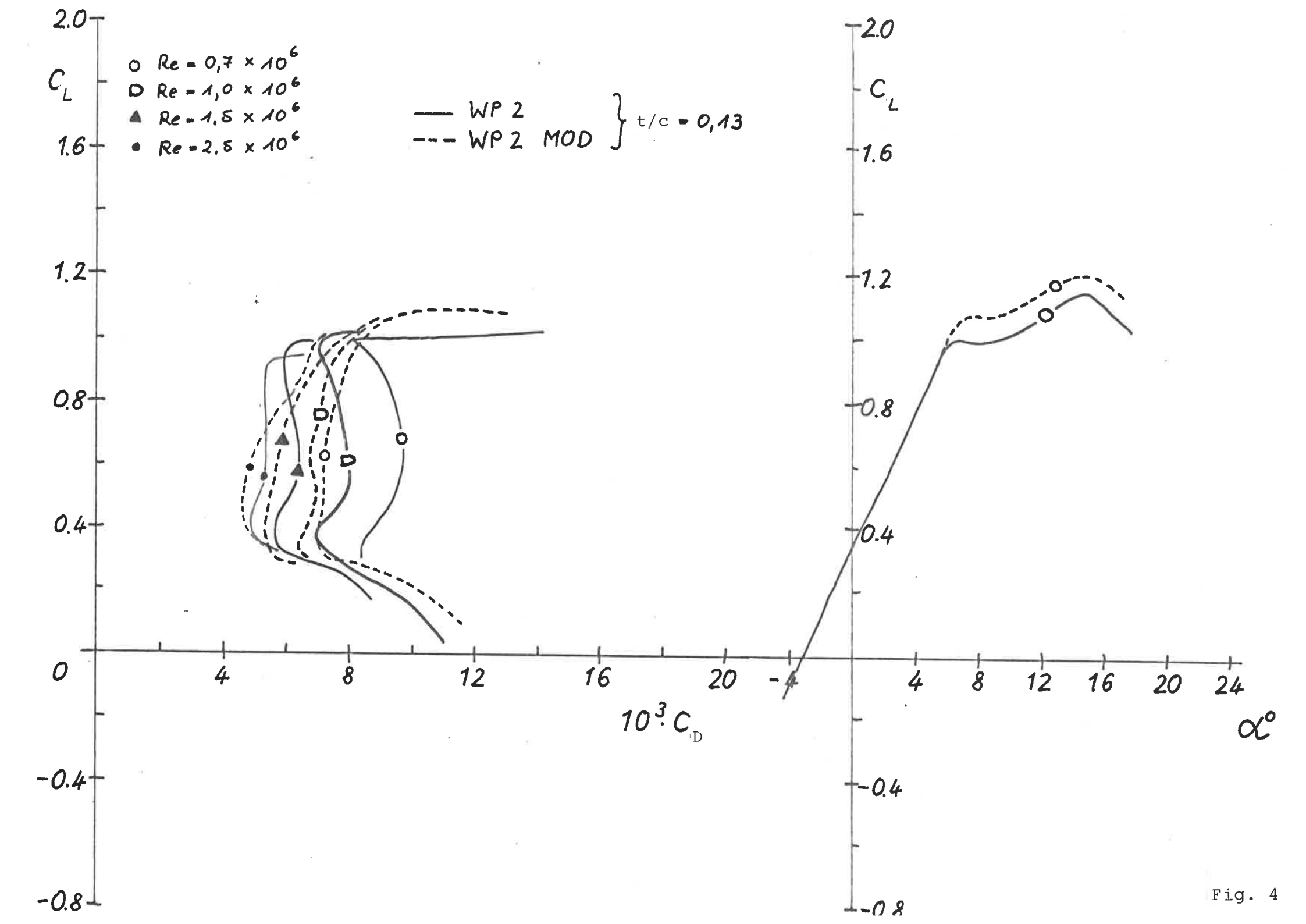
2.0
1.6
1.2
0.8
0.4
0
-0.4
-0.8
C_L
o Re = 0,7 x 10^6
D Re = 1,0 x 10^6
▲ Re = 1,5 x 10^6
• Re = 2,5 x 10^6
WP 2
WP 2 MOD
t/c = 0,13
4
8
12
16
20
$10^3 C_D$
-4
4
8
12
16
20
24
$\alpha°$

Fig. 4

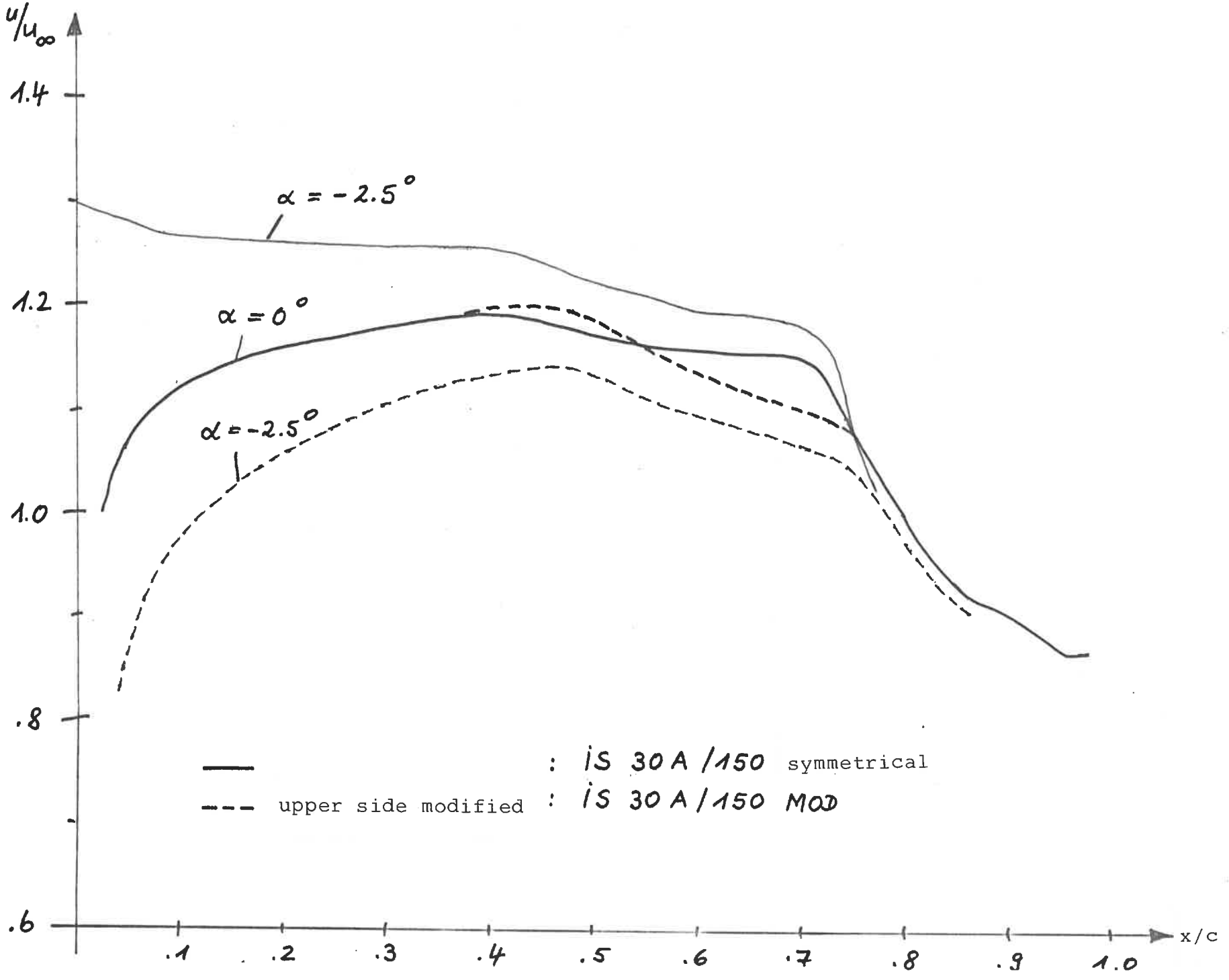
u/u∞
1.4
1.2
1.0
.8
.6
α = -2.5°
α = 0°
α = -2.5°
: IS 30 A /150 symmetrical
upper side modified : IS 30 A /150 MOD
.1
.2
.3
.4
.5
.6
.7
.8
.9
1.0
x/c

Fig. 5

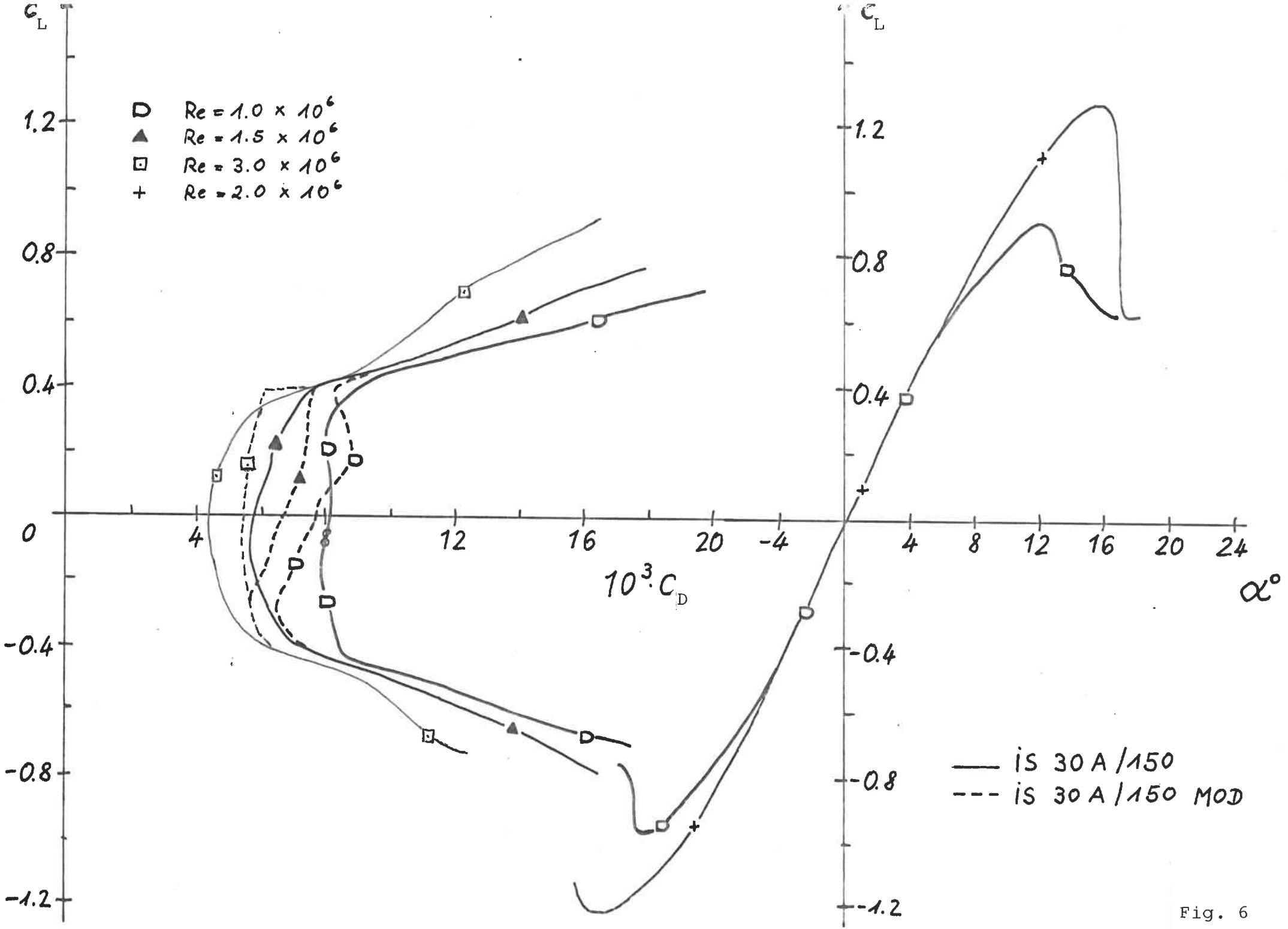
C_L
1.2
0.8
0.4
0
-0.4
-0.8
-1.2
Re = 1.0 × 10⁶
Re = 1.5 × 10⁶
Re = 3.0 × 10⁶
Re = 2.0 × 10⁶
4
8
12
16
20
-4
$10^3 . C_D$
C_L
1.2
0.8
0.4
-0.4
-0.8
-1.2
4
8
12
16
20
24
α°
IS 30 A /150
IS 30 A /150 MOD

Fig. 6

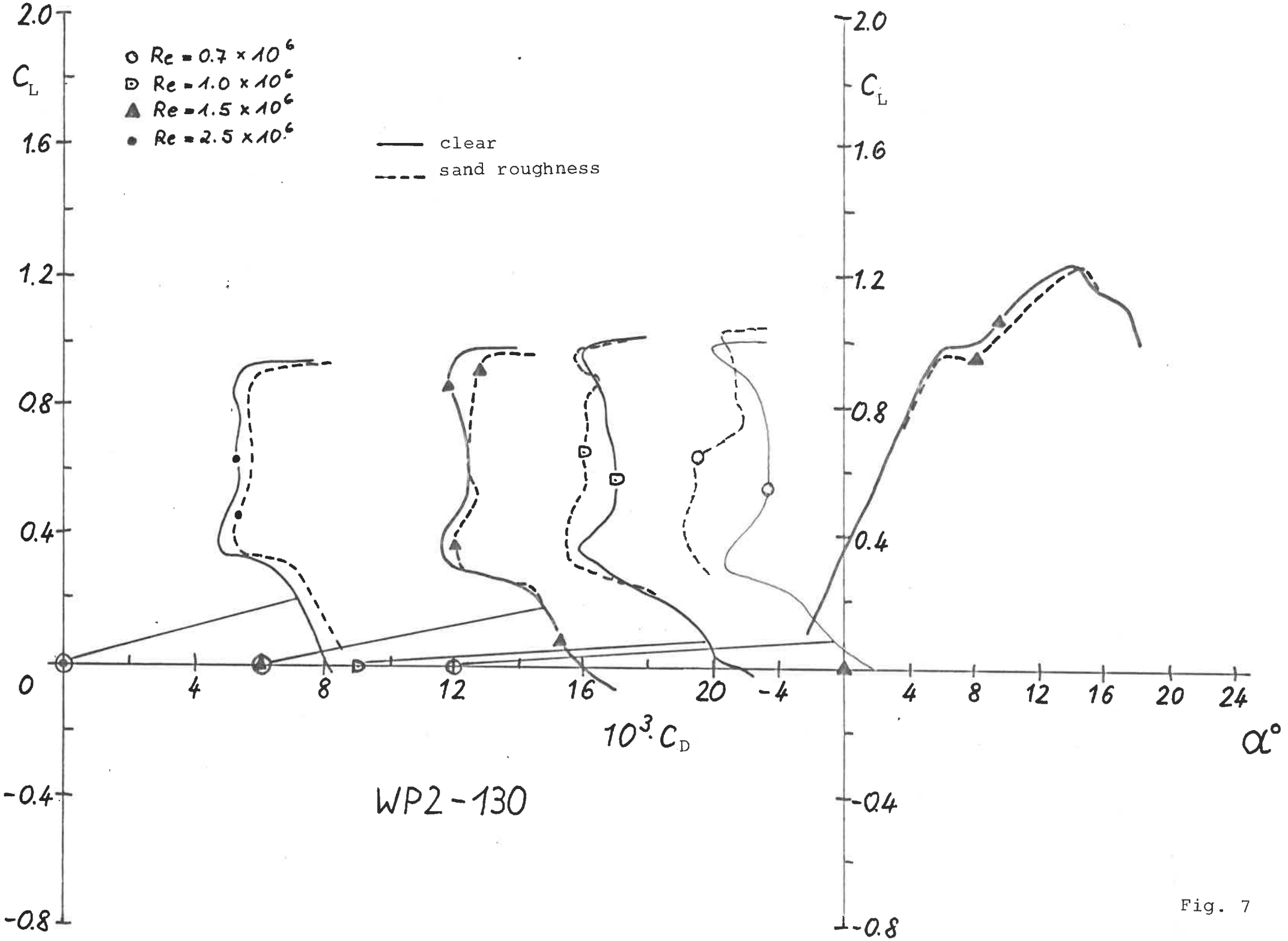
2.0
1.6
1.2
0.8
0.4
0
-0.4
-0.8
C_L
Re = 0.7 × 10⁶
Re = 1.0 × 10⁶
Re = 1.5 × 10⁶
Re = 2.5 × 10⁶
clear
sand roughness
4
8
12
16
20
-4
$10^3 . C_D$
WP2-130
4
8
12
16
20
24
α°

Fig. 7

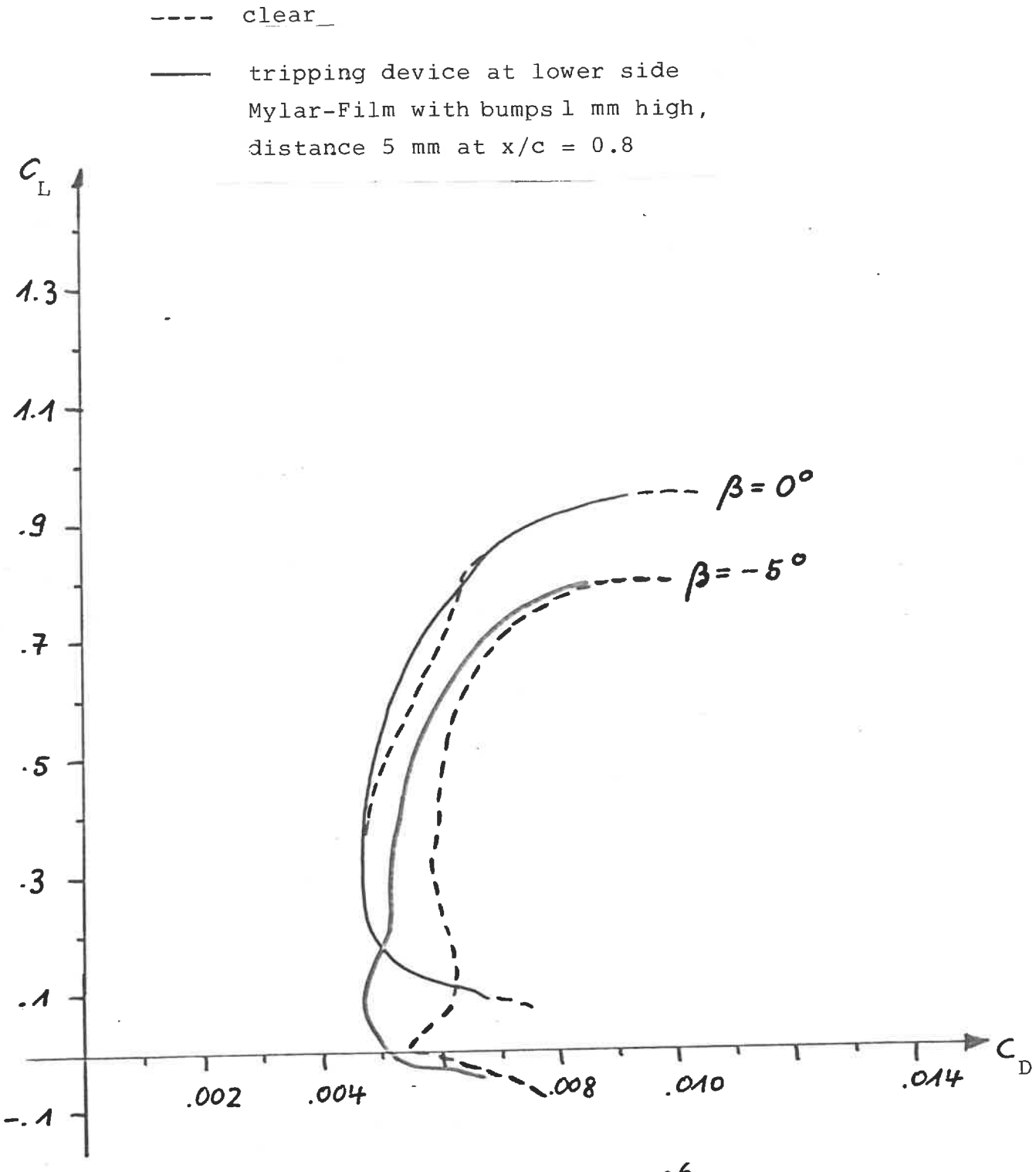
---- clear_
——— tripping device at lower side
Mylar-Film with bumps 1 mm high,
distance 5 mm at x/c = 0.8
C_L
1.3
1.1
.9
.7
.5
.3
.1
-.1
$\beta = 0°$
$\beta = -5°$
.002
.004
.008
.010
.014
C_D
t/c = 0.140
Re = 2.0 x 10⁶

Fig. 8

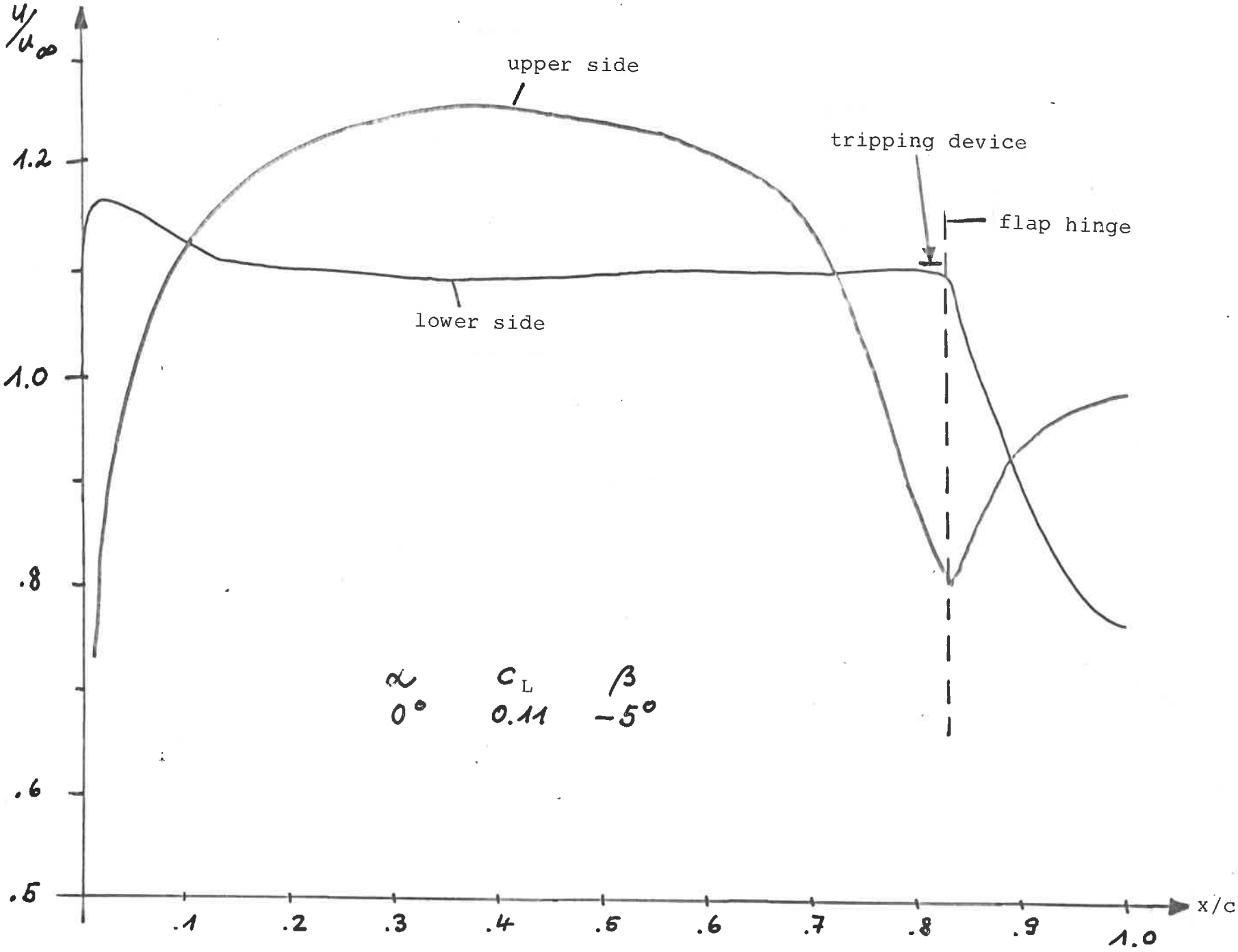
u/u∞
upper side
tripping device
flap hinge
lower side
1.2
1.0
.8
.6
.5
α
c_L
β
0°
0.11
−5°
.1
.2
.3
.4
.5
.6
.7
.8
.9
1.0
x/c

Fig. 9

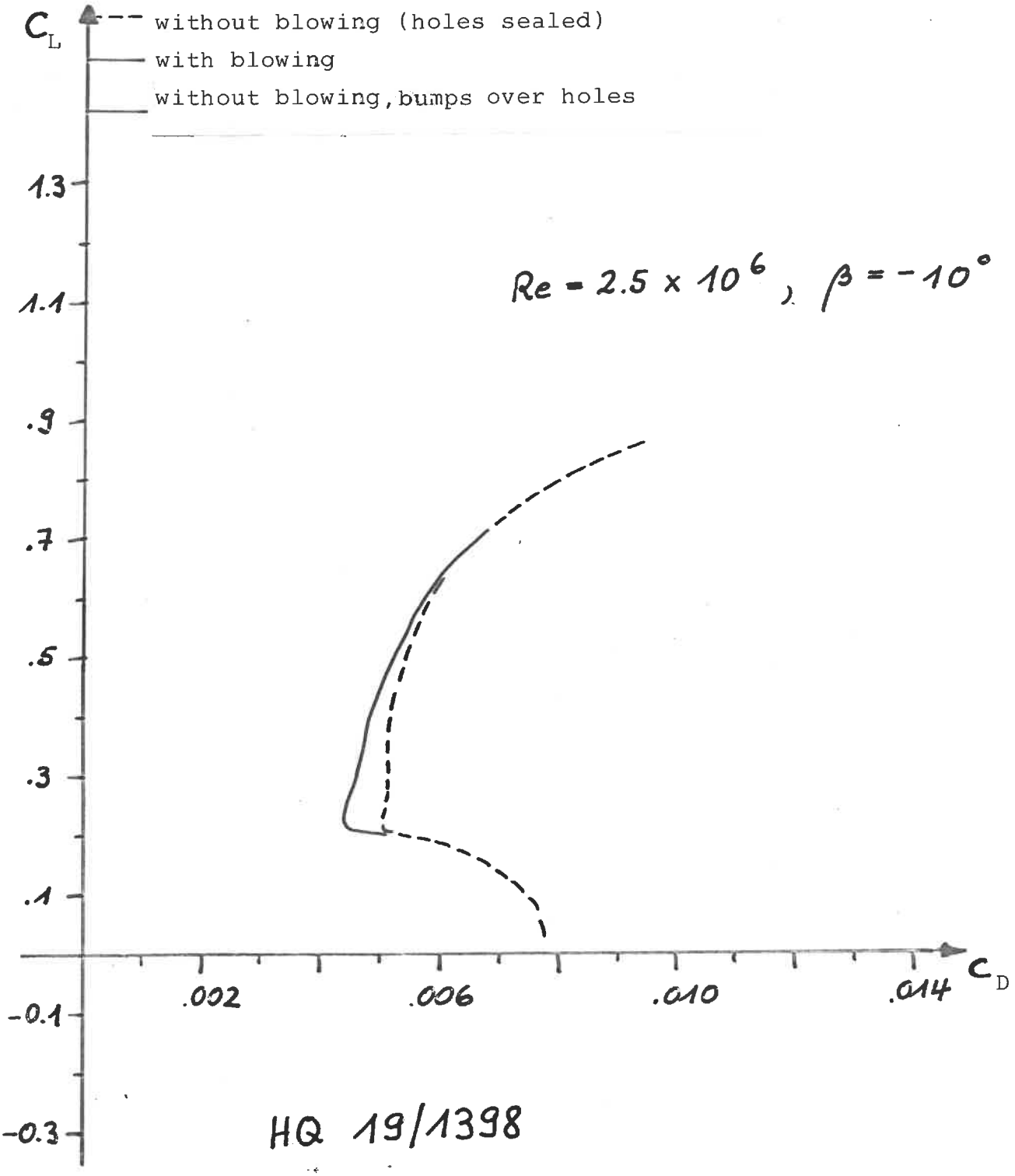
C_L
without blowing (holes sealed)
with blowing
without blowing, bumps over holes
1.3
1.1
.9
.7
.5
.3
.1
-0.1
-0.3
$Re = 2.5 \times 10^6$, $\beta = -10°$
.002
.006
.010
.014
C_D
HQ 19/1398

Fig. 10

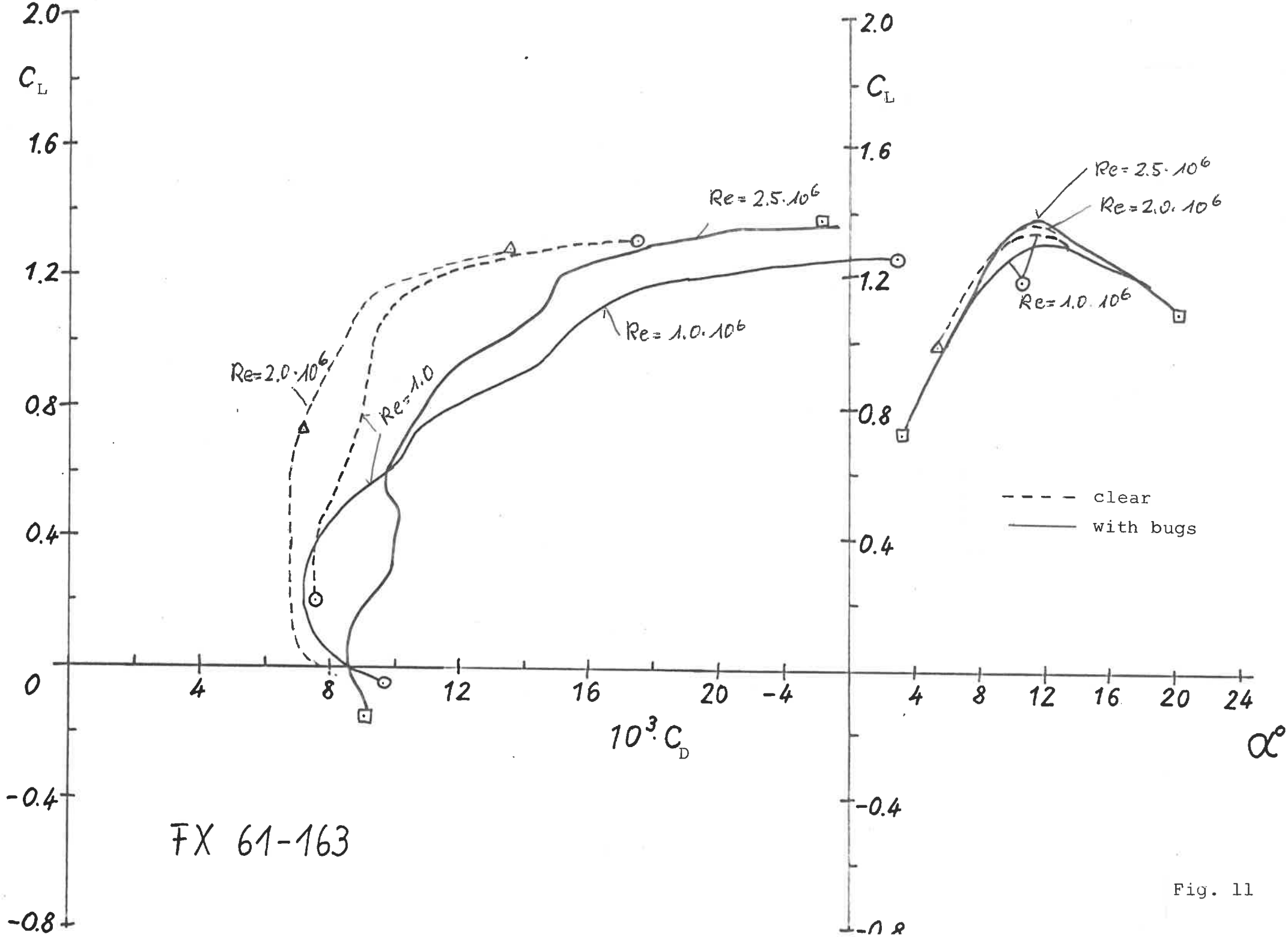
2.0
C_L
1.6
1.2
0.8
0.4
0
-0.4
-0.8
4
8
12
16
20
-4
$10^3 \cdot C_D$
Re = 2.5·10⁶
Re = 2.0·10⁶
Re = 1.0·10⁶
Re = 1.0
FX 61-163
2.0
C_L
1.6
1.2
0.8
0.4
-0.4
-0.8
4
8
12
16
20
24
$\alpha°$
Re = 2.5·10⁶
Re = 2.0·10⁶
Re = 1.0·10⁶
clear
with bugs

Fig. 11

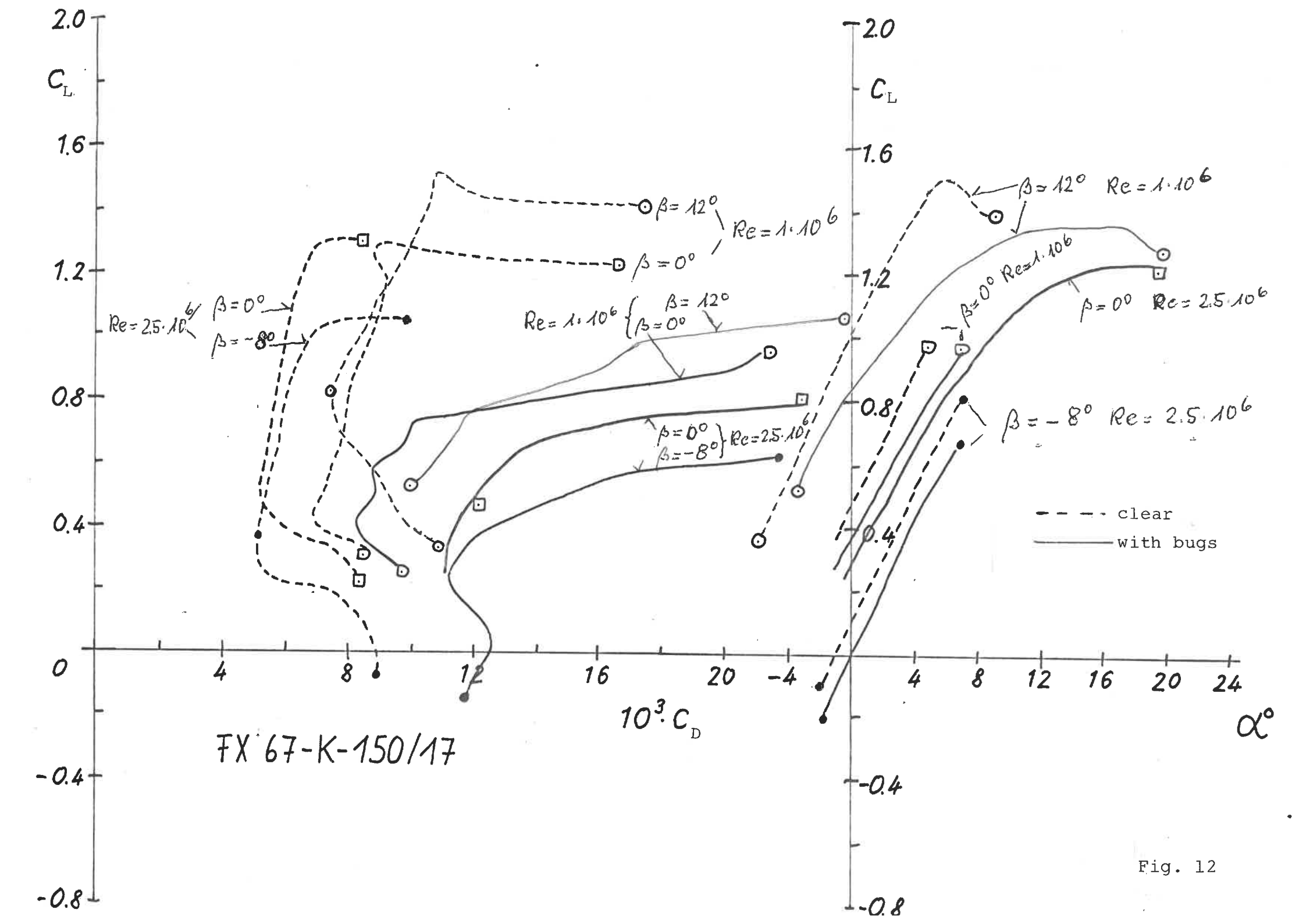
2.0
C_L
1.6
1.2
0.8
0.4
0
-0.4
-0.8
4
8
12
16
20
-4
$10^3 \cdot C_D$
$\alpha°$
FX 67-K-150/17
$\beta = 12°$
$\beta = 0°$
$Re = 1 \cdot 10^6$
$Re = 2.5 \cdot 10^6$
$\beta = -8°$
clear
with bugs

Fig. 12

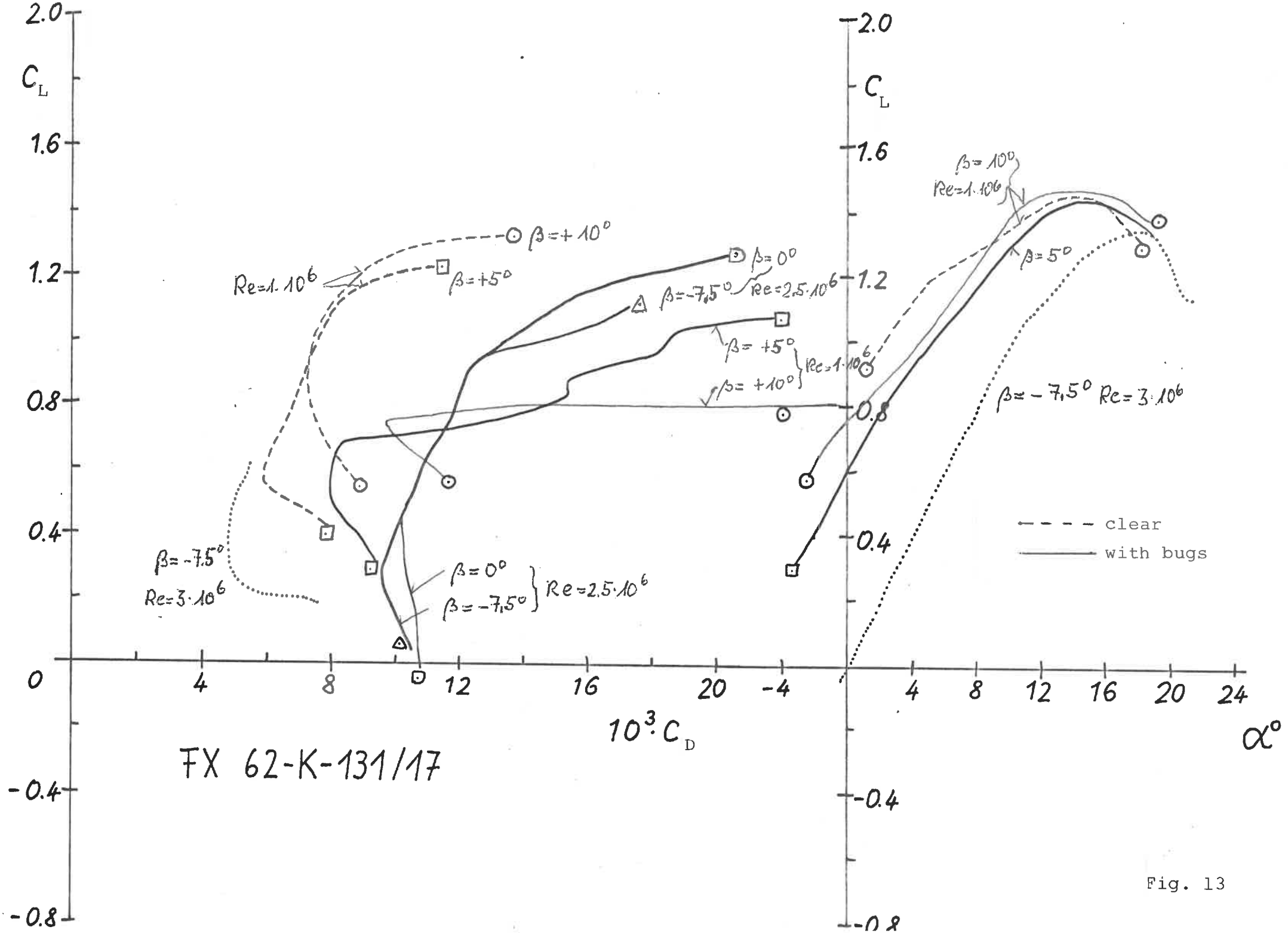
2.0
C_L
1.6
1.2
0.8
0.4
0
-0.4
-0.8
4
8
12
16
20
$10^3 C_D$
-4
4
8
12
16
20
24
α°
$\beta = +10^\circ$
$\beta = +5^\circ$
$Re = 1 \cdot 10^6$
$\beta = 0^\circ$
$\beta = -7,5^\circ$
$Re = 2,5 \cdot 10^6$
$\beta = +5^\circ$
$\beta = +10^\circ$
$Re = 1 \cdot 10^6$
$\beta = -7,5^\circ$
$Re = 3 \cdot 10^6$
$\beta = 0^\circ$
$\beta = -7,5^\circ$
$Re = 2,5 \cdot 10^6$
$\beta = 10^\circ$
$Re = 1 \cdot 10^6$
$\beta = 5^\circ$
$\beta = -7,5^\circ$ $Re = 3 \cdot 10^6$
clear
with bugs
FX 62-K-131/17

Fig. 13

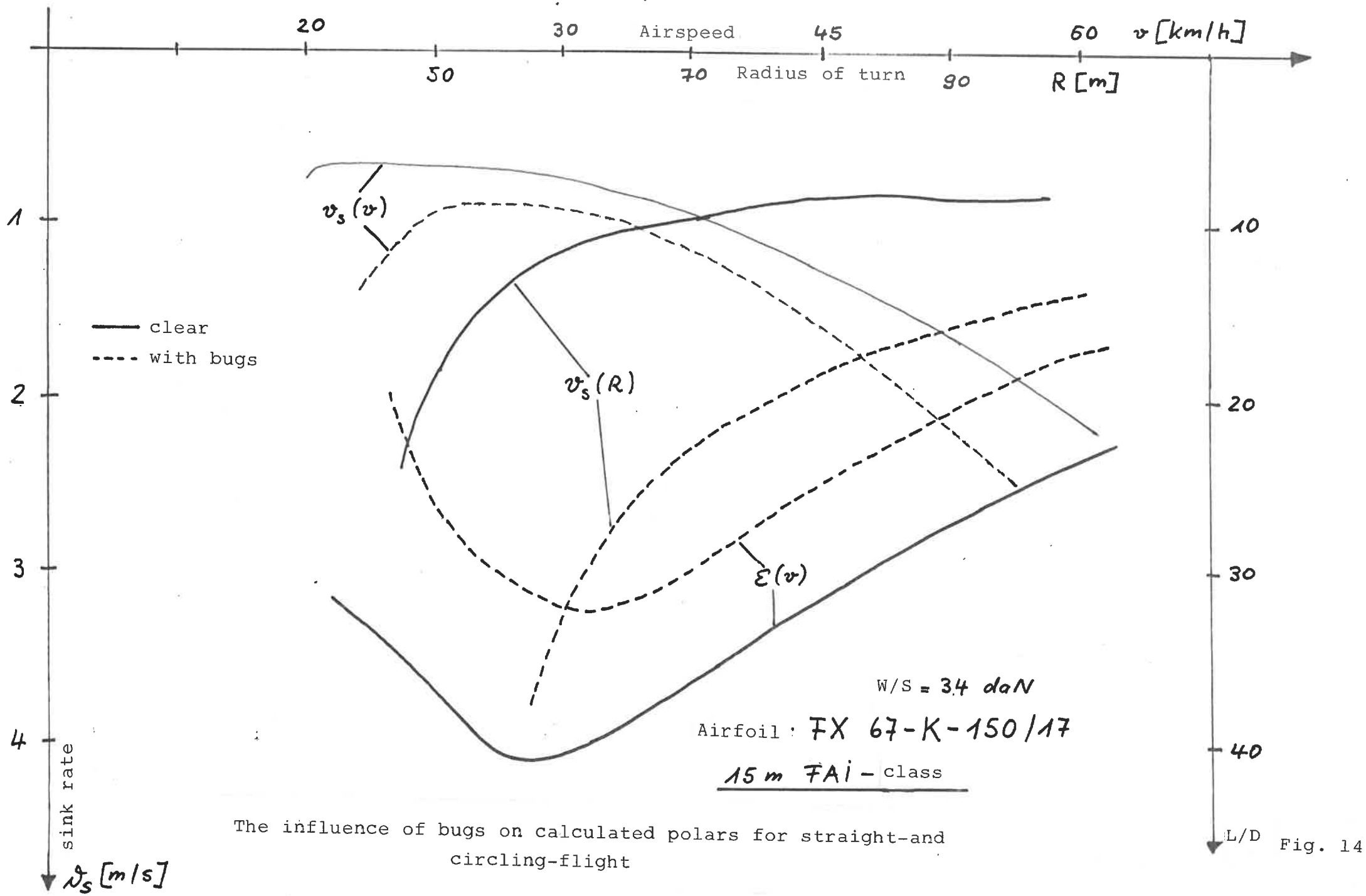

The influence of bugs on calculated polars for straight-and circling-flight

Fig. 14

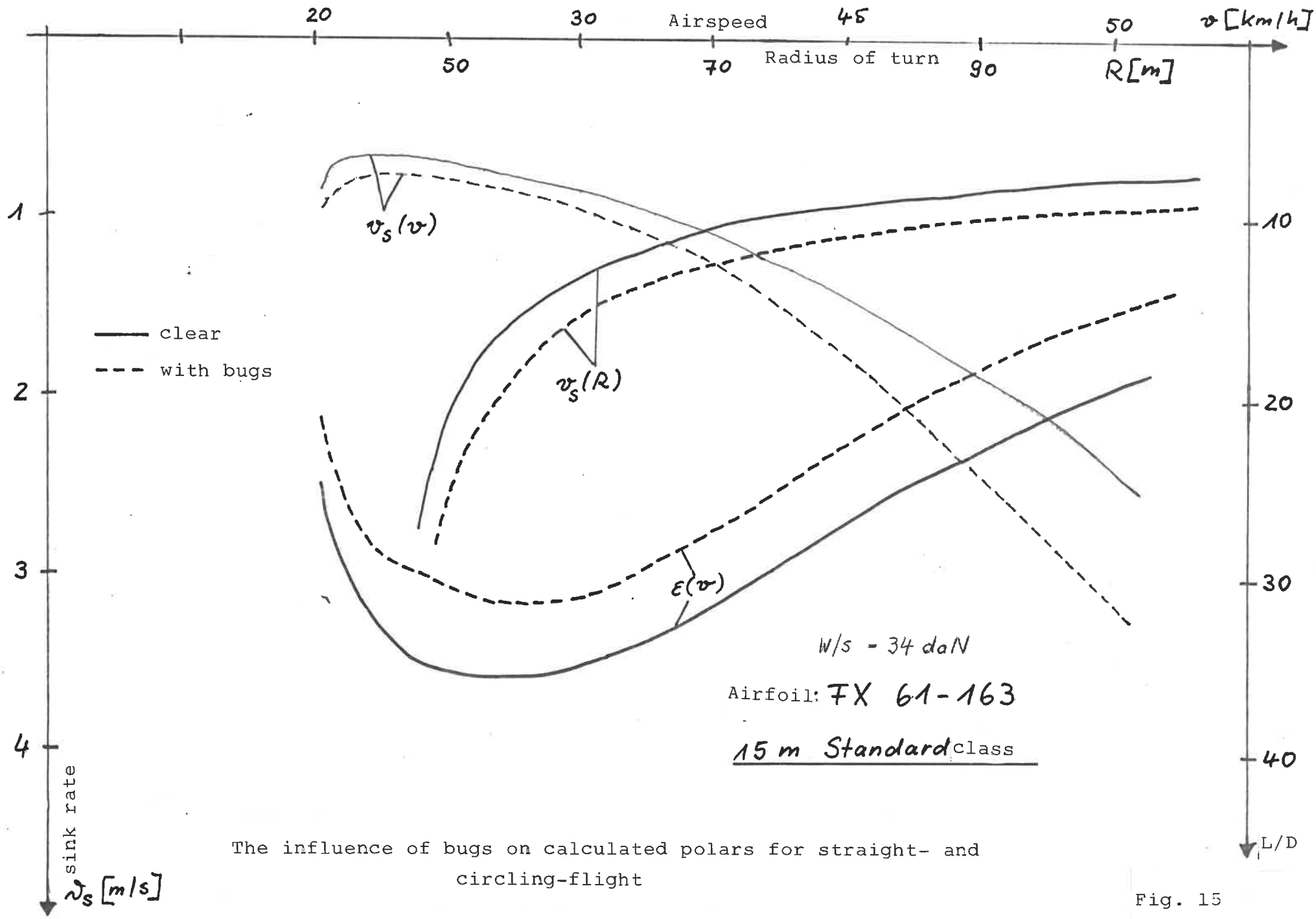

The influence of bugs on calculated polars for straight- and circling-flight

Fig. 15

W/S = 34 daN/m²	15m FAI - class FX 67-K-150/17			15 m Standard class FX 61-163		
	clear	bugs	%	clear	bugs	%
min. sink rate $v_{s\,min}$ [m/s]	0,66	0,91	+38	0,67	0,78	+16
opt. L/D $\varepsilon_{opt.}$	40,9	32,0	-22	35,8	32,0	-11
sink rate [m/s] at 110 [km/h]	0,75	0,94	+25	0,86	1,0	+16
sink rate [m/s] at 185 [km/h]	2,3	2,87	+25	2,6	3,37	+29
sink rate [m/s] at Radius 55 [m]	1,37	4,8	+250	1,57	1,89	+20
sink rate [m/s] at Radius 75 [m]	0,89	2,06	+131	0,98	1,17	+19
Radius of turn [m] at 1,5 [m/s] sinkrate	52	90	+73	55	62	+13
[km/h] cross country speed for a climb rate at 2 m/s	86	72	-16	82	76	-7

The influence of bugs on calculated performances of sailplanes

Table 1

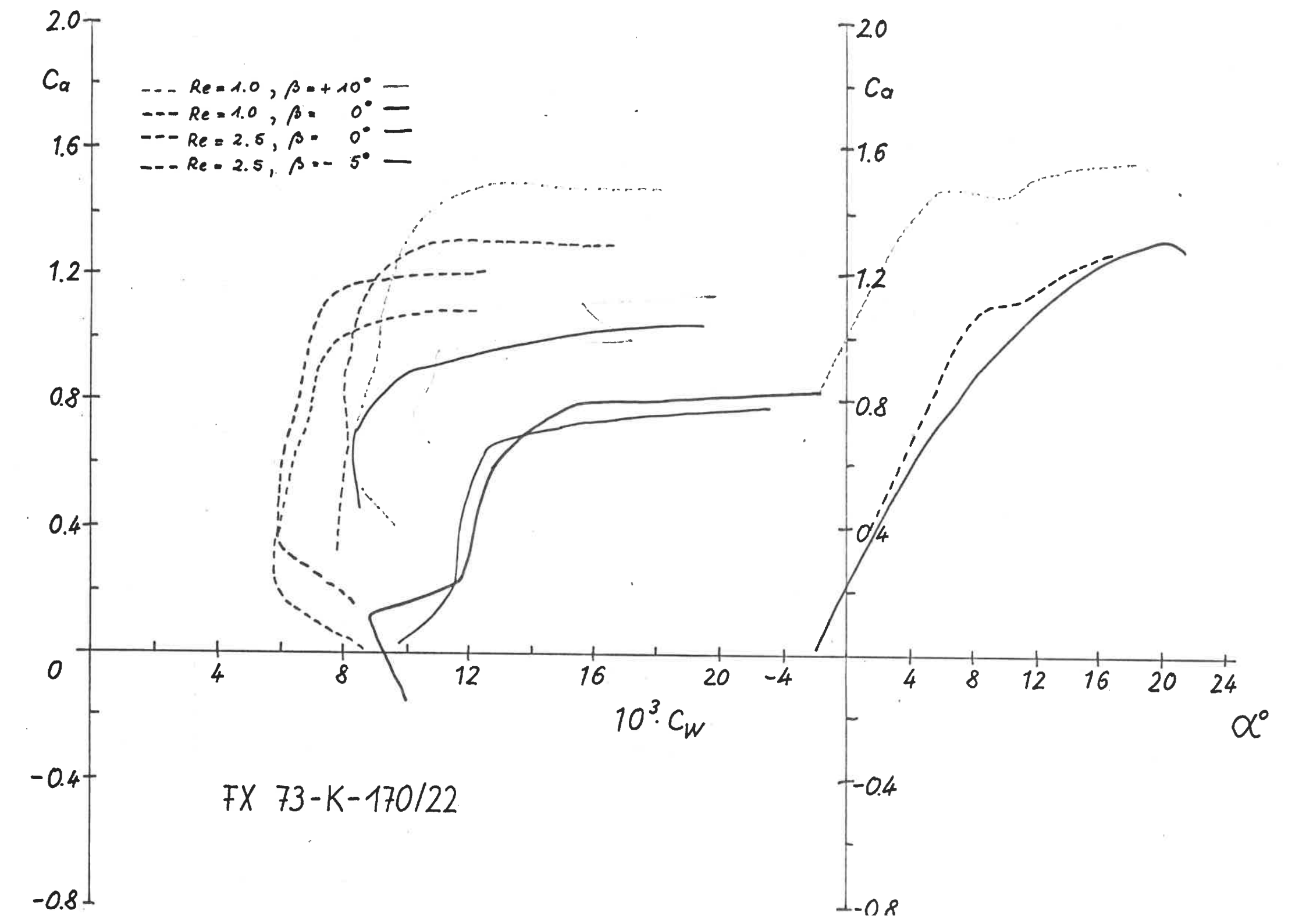
Ca
2.0
1.6
1.2
0.8
0.4
0
-0.4
-0.8
--- Re = 1.0 , β = + 10° —
--- Re = 1.0 , β = 0° —
--- Re = 2.5 , β = 0° —
--- Re = 2.5 , β = 5° —
4
8
12
16
20
-4
10³. Cw
Ca
2.0
1.6
1.2
0.8
0.4
-0.4
-0.8
4
8
12
16
20
24
α°
FX 73-K-170/22

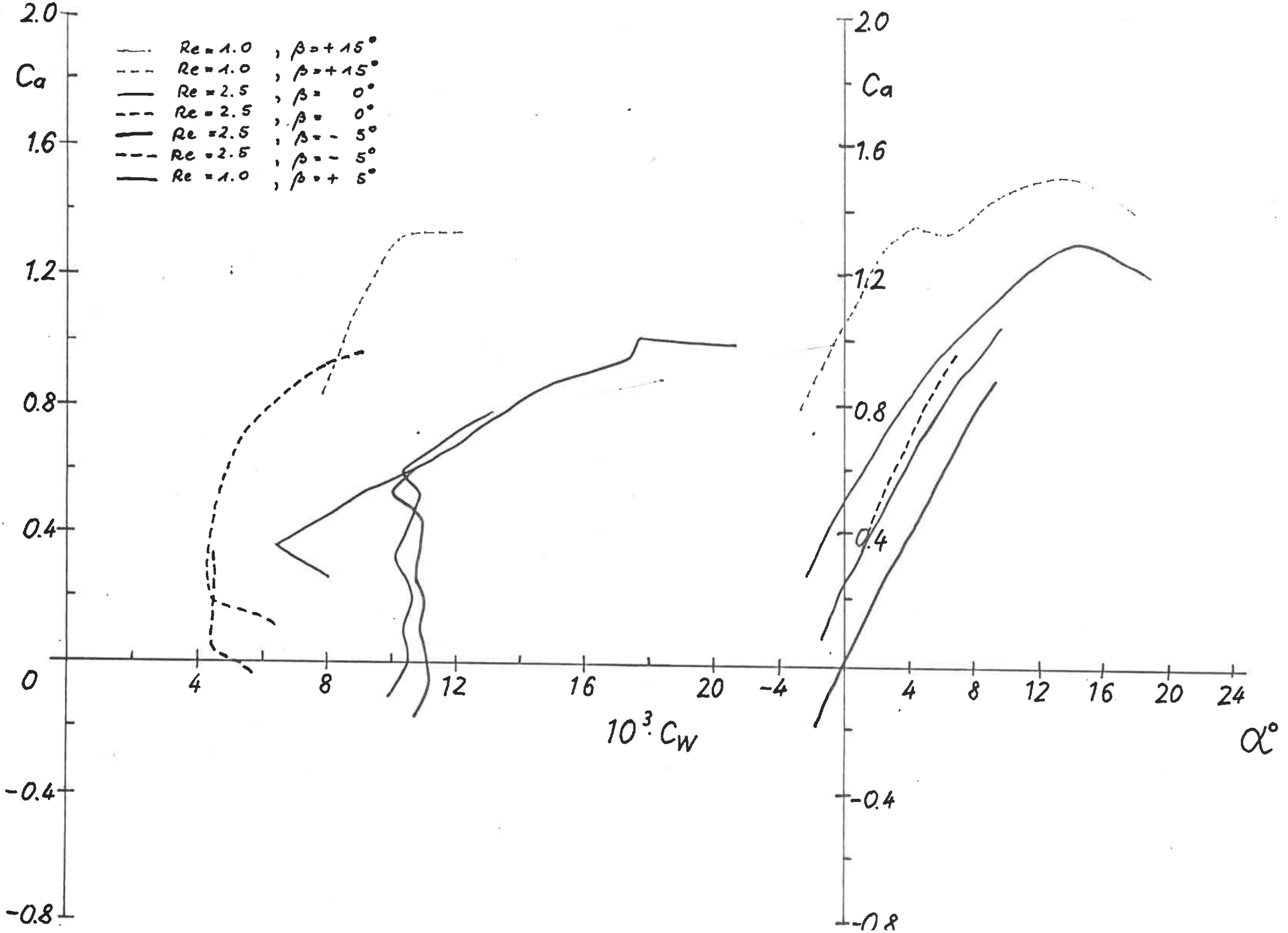
Re = 1.0 , β = + 15°
Re = 1.0 , β = + 15°
Re = 2.5 , β = 0°
Re = 2.5 , β = 0°
Re = 2.5 , β = - 5°
Re = 2.5 , β = - 5°
Re = 1.0 , β = + 5°
Ca
2.0
1.6
1.2
0.8
0.4
0
-0.4
-0.8
4
8
12
16
20
$10^3 \cdot C_W$
-4
Ca
2.0
1.6
1.2
0.8
0.4
-0.4
-0.8
4
8
12
16
20
24
α°

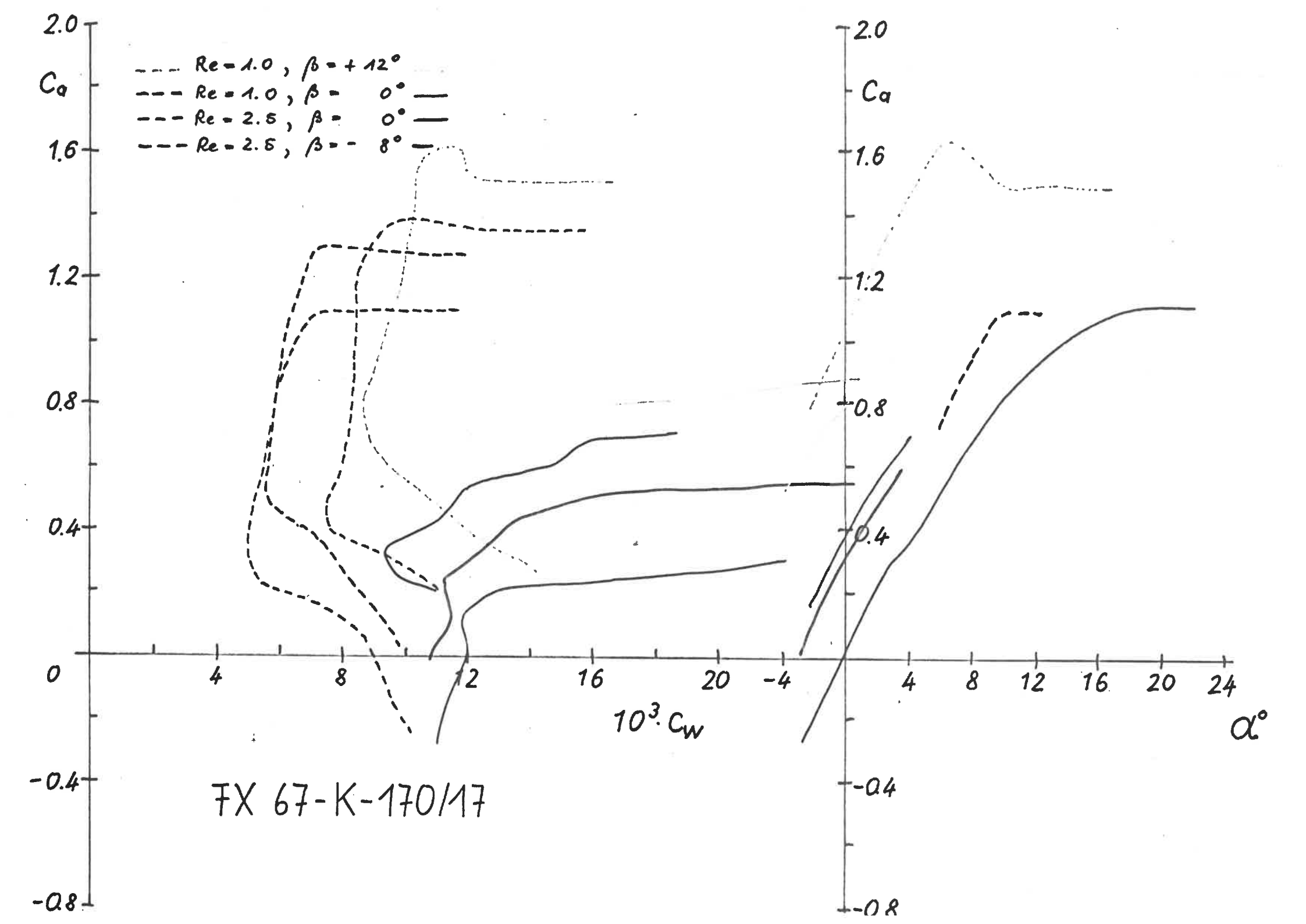
Re = 1.0 , β = + 12°
Re = 1.0 , β = 0°
Re = 2.5 , β = 0°
Re = 2.5 , β = - 8°
Ca
2.0
1.6
1.2
0.8
0.4
0
-0.4
-0.8
4
8
12
16
20
-4
10³ Cw
α°
24
FX 67-K-170/17